

Original Article

FeO*-Al₂O₃-TiO₂-Rich Rocks of the Tertiary Bana Igneous Complex, West Cameroon

Gilbert KUEPOUO^{1,*}, Hiroaki SATO², Jean-Pierre TCHOUANKOUE³ and Mamoru MURATA⁴

¹Department of Earth and Planetary Sciences, Graduate School of Science and Technology, Kobe University, Nada, Kobe, Japan

²Department of Earth and Planetary Sciences, Graduate School of Science, Kobe University, Nada, Kobe, Japan, ³Department of Earth Sciences, Faculty of Science, University of Yaounde-I, Yaounde, Cameroon, ⁴Department of Geosciences, Naruto University of Education, Naruto, Japan

Abstract

FeO*-Al₂O₃-TiO₂-rich rocks are found associated with transitional tholeiitic lava flows in the Tertiary Bana plutono-volcanic complex in the continental sector of the Cameroon Line. These peculiar rocks consist principally of iron-titanium oxides, aluminosilicates and phosphates, and occur as layers 1–3 m thick occupying the upper part of lava flows on the southwest (site 1) and northwest (site 2) sites of the complex. Mineral constituents of the rocks include magnetite, ilmenite, hematite, rutile, corundum, andalusite, sillimanite, cordierite, quartz, plagioclase, alkali feldspar, apatite, Fe-Mn phosphate, Al phosphate, micas and fine mixtures of sericite and silica. Texturally and compositionally, the rocks can be subdivided into globular type, banded type, and Al-rich fine-grained massive type. The first two types consist of dark globule or band enriched in Fe-Ti oxides and apatite and lighter colored groundmass or bands enriched in aluminosilicates and quartz, respectively. The occurrence of andalusite and sillimanite and the compositional relations of magnetite and ilmenite in the FeO*-Al₂O₃-TiO₂-rich rocks suggest temperatures of crystallization in a range of 690–830°C at low pressures. The Bana FeO*-Al₂O₃-TiO₂-rich rocks are characterized by low concentrations of SiO₂ (25–54.2 wt%), Na₂O + K₂O (0–1%), CaO (0–2%) and MgO (0–0.5%), and high concentrations of FeO* (total iron as FeO, 20–42%), Al₂O₃ (20–42%), TiO₂ (3–9.2%), and P₂O₅ (0.26–1.30%). TiO₂ is positively correlated with Al₂O₃ and inversely correlated with FeO*. The bulk rock compositions cannot be derived from the associated basaltic magma by crystal fractionation or by partial melting of the mantle or lower crustal materials. In ternary diagrams of (Al₂O₃)-(CaO + Na₂O + K₂O)-(FeO* + MnO + MgO) and (SiO₂)-(FeO*)-(Al₂O₃), the compositional field of the rocks is close to that of laterite and is distinct from the common volcanic rocks, suggesting that the rocks are derived from lateritic materials by recrystallization when the materials are heated by the basaltic magmas. A hydrothermal origin is discounted because the rocks contain high-temperature mineral assemblages and lack sulfide minerals. It is proposed that the FeO*-Al₂O₃-TiO₂-rich rocks of the Bana complex were formed by pyrometamorphism of laterite by the heat of basaltic magmas.

Keywords: Bana igneous complex, Cameroon Line, Fe-oxide ores, FeO*-Al₂O₃-TiO₂-rich rocks, laterite.

1. Introduction

Peculiar rocks with high concentrations of iron oxides and alumina were found in the Tertiary Bana igne-

ous complex of West Cameroon. They occur as massive rocks and are associated with lava flows of transitional tholeiitic basalts (Kuepouo *et al.*, 2006). The rocks are dense and have a submetallic luster sometimes with

Received 16 February 2007. Accepted for publication 3 April 2008.

Corresponding author: H. SATO, Department of Earth and Planetary Sciences, Graduate School of Science, Kobe University, Rokko-dai 1-1, Nada-ku, Kobe 657-8501 Japan. Email: hsato@kobe-u.ac.jp

*Present address: Department of Earth Sciences, Faculty of Science, University of Yaounde-I, Yaounde, Cameroon

strong magnetism due to the presence of abundant magnetite. The rocks differ from other occurrences of iron oxide ores associated with volcanic rocks by simultaneous enrichment of alumina. Iron oxide apatite ores associated with volcanic rocks are reported worldwide: the El Laco deposit, Chile, situated on the flanks of an andesite-rhyodacite volcano, consists chiefly of magnetite, hematite and apatite (Park, 1961); the Kiruna deposit, Northern Sweden, which constitutes the greatest apatite-iron ore in the world occurring in intermediate volcanic rocks, also consists typically of magnetite, hematite and apatite (Frietsch, 1978). Both magmatic and hydrothermal origins were advocated for these iron oxide-apatite ores (e.g. Nystrom & Henriquez, 1994; Edfelt *et al.*, 2005). The FeO* (total iron as FeO)-Al₂O₃-TiO₂-rich rocks we report here have some similarities to the iron oxide-apatite ores in petrography and geochemistry, although the presence of abundant Al minerals is distinctive and may have a different origin. The aims of the present study were to describe the geology, petrography and geochemistry of the FeO*-Al₂O₃-TiO₂-rich rocks from the Tertiary Bana igneous complex, West Cameroon, to discuss their origin, and comment on their relevance to ore-geology debate concerning the origin of magnetite-apatite ore deposits.

2. Geological setting of the FeO*-Al₂O₃-TiO₂-rich rocks

The Bana igneous complex is located in the central part of the Cameroon Line, a typical within-plate magmatic province straddling the oceanic and continental plates in central Africa (inset of Fig. 1) (Fitton, 1987). The continental sector of the Cameroon Line is built on a thin crust approximately 20–30 km thick, which is 10 km thinner compared with the crustal thickness out of the line (Poudjom Djomani *et al.*, 1995, 1997). Moreau *et al.* (1987) regarded the continental sector of the Cameroon Line as a Pan-African paleosuture. The Bana igneous complex occupies an area 4 × 7 km, intruding/abutting against Pan African granite and gneisses (Toteu *et al.*, 1994) to the south and surrounded by Tertiary flood basalt to the west, north and east. The complex consists of plutonic rocks of syenodiorite, alkalic granite and calc-alkalic granite, and of volcanic rocks of alkalic rhyolite, quartz trachyte, FeO-Al₂O₃-TiO₂-rich rocks, transitional plagioclase-phyric basalts, benmoreite to rhyolitic welded tuffs and basanite, alkalic olivine basalt and hawaiite (Fig. 1) (Kuepouo, 2004). The FeO*-

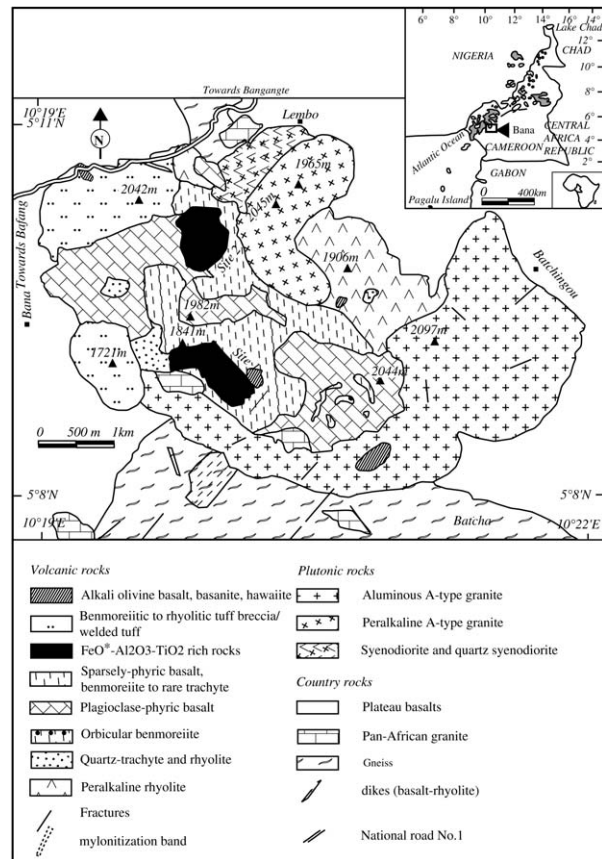


Fig. 1 Geological map of Bana Igneous Complex, west Cameroon (Kuepouo, 2004).

Al₂O₃-TiO₂-rich rocks are contiguous to lava flows of transitional tholeiitic basalts and subordinate benmoreite and trachytes in the Tertiary Bana igneous complex. The transitional tholeiitic basalts top the central part of the weakly peralkalic granite in the south and are locally roofed by basaltic lapilli, trachyte and rhyolites. K-Ar age of the plagioclase phenocrysts in the transitional tholeiitic basalts is 30.1 ± 1.2 Ma (Kuepouo *et al.*, 2006).

The FeO*-Al₂O₃-TiO₂-rich rocks are located in the southwest (site 1) and northwest (site 2) of the Bana igneous complex. These two sites are 2 km apart, separated by plagioclase-phyric and sparsely phyric transitional tholeiitic basalts. The FeO*-Al₂O₃-TiO₂-rich rocks cover a surface area of approximately 1000 m × 500 m and 750 m × 500 m in sites 1 and 2, respectively (Fig. 1). Each site is similar in size to the Laco Norte iron deposit, Chile (Naslund *et al.*, 2002). These FeO*-Al₂O₃-TiO₂-rich rocks are conspicuous because of their rusty weathering. They differ from common fine-grained

basalt by their high density, mode of alteration, submetallic luster (the iron-rich varieties), coarse “globular” and banded structures and their black–brown color. Some of the iron-rich varieties show strong magnetism. The FeO*-Al₂O₃-TiO₂-rich rocks are fine-grained. Three textural types of the FeO*-Al₂O₃-TiO₂-rich rocks can be distinguished: iron-rich globular type, which is the most abundant among the three types; iron-rich banded type; and fine-grained massive Al-rich type. The iron-rich globular type varies from black to brownish in color. Globules form the darker parts of this type. Globules are generally rounded to irregular with diameters of several millimeters to a few centimeters (Fig. 2c). Ratio of globule to matrix ranges from 2:1 to 1:2. In the second type, the iron-rich bands are always brownish

and are mineralogically similar to globules. The iron-rich dark band alternate with white band and their thickness ranges from 1 to 15 mm (Fig. 2d). The modal ratio of dark and white bands in the second type is from 1:1 to 1:2. In the third type, fine-grained Al-rich types have the same texture as iron-poor and Al-rich groundmass and iron-poor and Al-rich bands in globular and banded types of the FeO*-Al₂O₃-TiO₂-rich rocks, respectively. Subtle banded textures outlined by parallel array of elongated spots typically 1 mm thick and up to 3 mm long of slightly different color are common in the third type.

In places the FeO*-Al₂O₃-TiO₂-rich rocks are blocky jointed (Fig. 2a). Some traverses upstream (Fig. 2b) suggest that each flow consists of two distinct zones:



Fig. 2 Occurrence of the FeO*-Al₂O₃-TiO₂-rich rocks in the Bana complex. (a) Massive globular-type FeO*-Al₂O₃-TiO₂-rich rocks occupy the outcrop, northern body. (b) Occurrence of massive brown Al-rich rocks overlying the basaltic lava flow. (c) Close-up of a polished slab of the globular type FeO*-Al₂O₃-TiO₂-rich rocks, showing sharp boundary between the globules (Glo) and groundmass (Gr). Bar, 1 cm. (d) Block of banded-type FeO*-Al₂O₃-TiO₂-rich rocks in the southern body.

an upper loose, prismatic or blocky part consisting of iron-rich globular and subsidiary banded types 0.5–2 m thick; and a lower, massive part consisting of compact and locally prismatic Al-rich lava locally up to 3 m thick. The iron-rich zone seems to thicken toward the axial part of the flow. Occasionally, small vesicles are found in some globules. The adjacent volcanic rocks and the FeO*-Al₂O₃-TiO₂-rich rocks are exposed at a similar structural level, and the base of the rocks was not available for observation. The traverses between volcanic rocks and the FeO*-Al₂O₃-TiO₂-rich rocks do not show any irregular mixture or the presence of soil between them. Locally the contact is fracture-controlled surface resembling cooling-related cracks (Fig. 2b). Neither veining nor alteration were observed within the FeO*-Al₂O₃-TiO₂-rich rocks and contact rocks.

3. Petrography and mineral chemistry

Mineral compositions were obtained on electronprobe microanalysis (JEOL JX8900) at the Venture Business Laboratory of Kobe University, operating at 15 kV and 12 nA using the wavelength dispersive system (WDS), focused beam and 6–80s peak counting times. Standards used were as follows: Si, SiO₂; Al, Al₂O₃; Na and Cl, NaCl; Mg, MgO; Ti, TiO₂; Fe, Fe₂O₃; Mn, MnO; Ca, CaSiO₃; K, natural adularia; P, natural apatite; F, fluorite. ZAF corrections were made on the background-corrected raw counting data to produce the weight percent of elements.

The Bana FeO*-Al₂O₃-TiO₂-rich rocks generally have aphyric texture, and the major mineral assemblage of the globule and matrix in the globular type are almost the same. This is confirmed on both X-ray diffraction and electronprobe microanalysis. The main constituent minerals of the globular and banded types are quartz, andalusite, cordierite, titanomagnetite, ilmenite, apatite and feldspars. Minor or local occurrences are noted for hematite, rutile, corundum, sillimanite, metakalinite, iron-mangano-phosphates, aluminous phosphate, and sericite. The crystals are fine-grained, commonly 10–50 μm in diameter, although in some globules the individual minerals, chiefly apatite and titanomagnetite, are up to 1.5 mm across (Fig. 3a). Large apatite crystals may poikilistically include crystals of ilmenite and/or titanomagnetite. A fluid texture is sometimes observed in the FeO*-Al₂O₃-TiO₂-rich rocks (Fig. 3b). This is represented by parallel alignment of fine-grained rectangular aluminosilicates, somewhat similar to pilotaxitic texture of volcanic

rocks, and is found in the matrix of Fe-rich parts (globules or Fe-rich band) of the FeO*-Al₂O₃-TiO₂-rich rocks. Figure 3(a) shows such an example, where the dark part consisting of andalusite and silica is embedded in Fe-Ti oxide matrix. Locally some samples contain chiefly hematite and titanohematite. Some of this hematite and titanohematite has a micro-vein network of apatite composition. Apart from the occurrences of rare microphenocrysts of sodic plagioclase in Al-rich lavas, these lavas have the same mineral composition and proportion as iron-poor and Al-rich groundmass, and iron-poor and Al-rich bands of globular and banded types, respectively. Al-rich lavas have a finely globular texture toward the upper iron-rich FeO*-Al₂O₃-TiO₂-rich rocks and become very fine-grained to spherulitic in texture toward their edges. The size of the faint globules is sometimes up to 20 cm in diameter. Albite, sanidine, andalusite are often altered to fine-grained mass of sericite.

The magnetite and titanomagnetite (Table 1; Fig. 5) have compositions ranging from Usp₆₅Mt₃₅ to nearly pure magnetite, although they contain fairly high Al₂O₃ content up to 40% hercynite. Spinel has continuous solid solutions within the system FeO-Fe₂O₃-Al₂O₃ at temperatures >800°C (Turnock & Eugster, 1962), implying that this assemblage is primary in the paragenesis.

Ilmenite in the FeO*-Al₂O₃-TiO₂-rich rocks has very low MgO <0.07 wt% and MnO <0.5 wt% content. It is almost continuous in composition from ilmenite to hematite (Table 1; Fig. 5). Ilmenite or “ferro-pseudobrookite” may occur in the core of titanomagnetite crystals. There occurs symplectites of either rutile + ilmenite, or rutile + titanomagnetite approximately 50–200 μm across. The symplectites consist of thin vermicular blebs of rutile several microns thick and 10–20 μm long embedded in either ilmenite or titanomagnetite. Defocused beam (5–10 μm across) analyses of the symplectites show that they have 59–70 wt% TiO₂ (Fig. 5), and may represent the pseudomorph of ferro-pseudobrookite.

Idiomorphic corundum was found associated with andalusite in an Al-rich groundmass of globular type FeO*-Al₂O₃-TiO₂-rich rocks. The corundum crystals are idiomorphic, 50–200 μm long and 10–30 μm wide (Figs. 3d, 4). They are wholly or partly included in titanomagnetite, and also contact with allotriomorphic andalusite. Corundum and quartz are present in a thin section but are not in contact, and andalusite and cordierite are present between these minerals (Figs. 3d, 4). Andalusite is sometimes idiomorphic (Fig. 3c) and

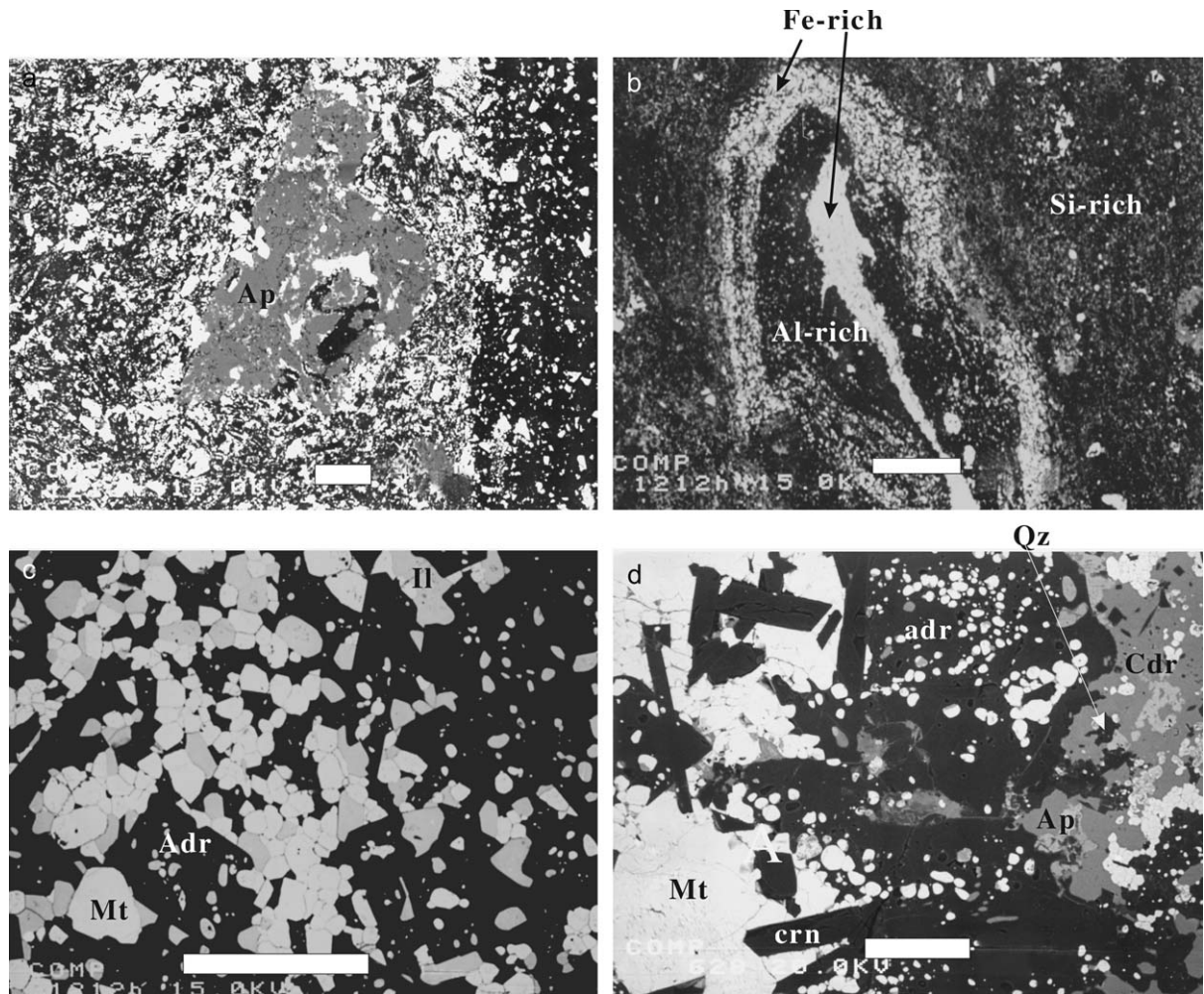


Fig. 3 Back-scattered electron images of the FeO*-Al₂O₃-TiO₂-rich rocks. Bars, 100 μ m. (a) Fine-grained globule on the left and groundmass in the right margin. Phenocryst of apatite is notable in the globule. The globular part shows parallel arrangement of fine-grained oxide and interstitial andalusite and silica minerals. Sample No. K117. (b) Folded texture of iron-rich band in sample K113. (c): Enlarged view of the globular part, consisting of euhedral-subhedral titanomagnetite, ilmenite and andalusite with interstitial metakaolinite and silica minerals in sample K-111. (d) Occurrence of idiomorphic corundum (dark elongated crystal) partly or wholly embedded in large magnetite in the left part of the photo. Central dark area is mostly composed of andalusite together with minor amounts of cordierite, K-feldspar and quartz. Intermediate bright area in the right part of the photo includes Ca apatite, Fe-Mn apatite, cordierite and quartz. K-105.

sometimes anhedral, and has stoichiometric compositions with 1–3 wt% FeO* (Table 2). Sillimanite locally occurs as fibrolite with characteristic optical properties in the Al-rich matrix of the rocks. Cordierite occurs as irregularly shaped crystal and has a high Fe/(Mg + Fe) ratio of 0.65–0.66. Plagioclase has a Ca/(Ca + Na) ratio of 0.17–0.22. Quartz and amorphous silica are ubiquitous, but are mostly anhedral. Quartz contains minor amounts of FeO* and Al₂O₃ (Table 2). Amorphous silica shows some compositional variation with 3–5 wt% of Al₂O₃, and lacks total deficiency, suggesting that it is

anhydrous. An unidentified alumina phase has a total range of Al₂O₃ between 89 and 92 wt%. Appreciable amounts of FeO* and SiO₂ are also present (Table 2), and suggest that the unidentified alumina phase is actually mixed crystals of corundum, iron oxides and silica minerals. The total oxide sum converges to approximately 100 wt%, suggesting that the aluminous minerals in the FeO*-Al₂O₃-TiO₂-rich rocks are anhydrous. A white band of the banded type rocks contains abundant mica and aluminosilicates. The crystals are fibrous and have high birefringence. The chemical

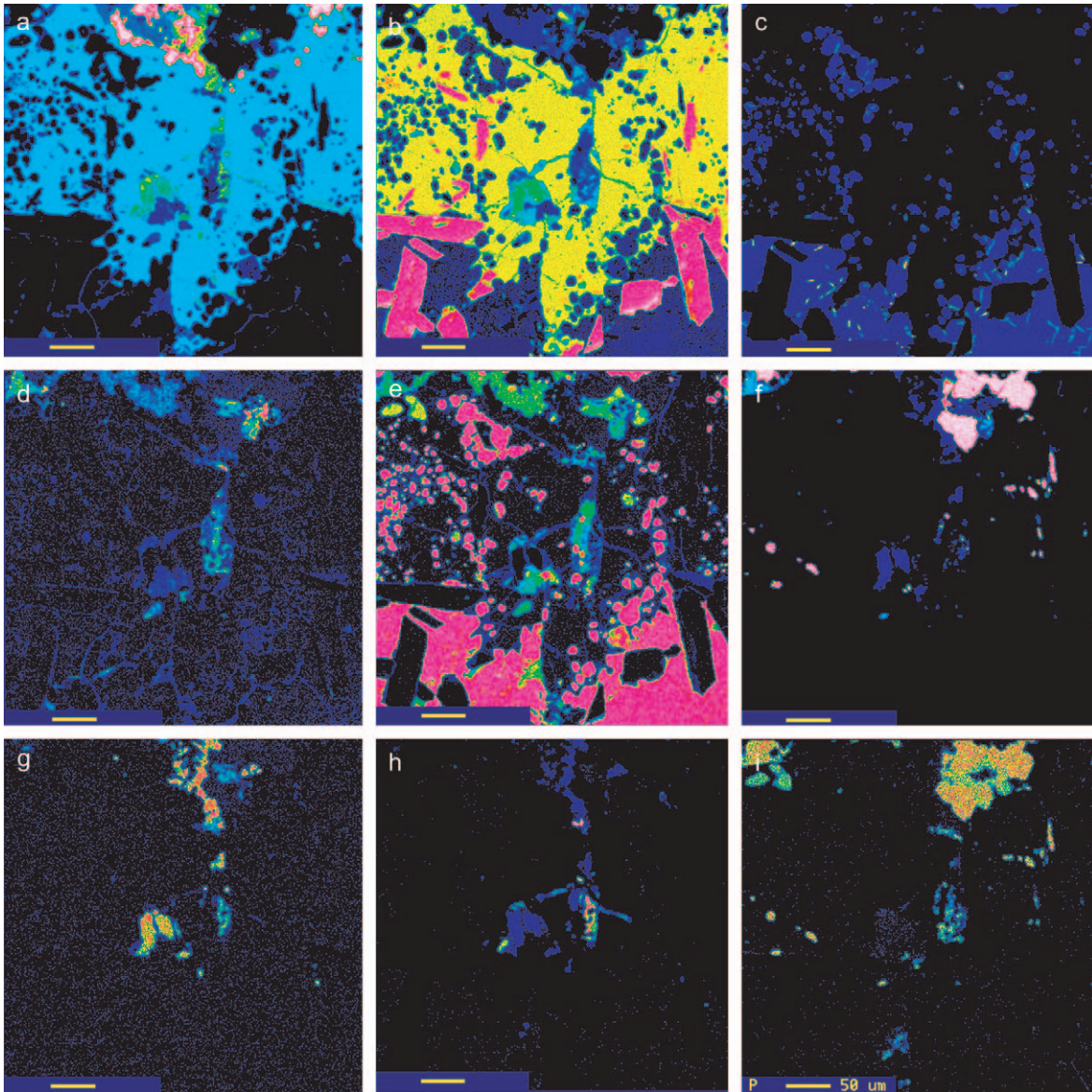


Fig. 4 X-ray mapping of a portion of the globular-type FeO*-Al₂O₃-TiO₂-rich rocks, K-105. Corundum: red in (b) Al map; magnetite with ilmenite lamellae: red in (e) Fe map; andalusite: light blue in (a) Si map; cordierite: green in (e) Fe map; quartz: red in (a) Si map; plagioclase: yellow-orange in (g) Na map; alkali feldspar: yellow-orange in (h) K map; apatite: red white in (f) Ca map; Fe phosphate: yellow in (e) Fe map. (c) Ti; (d) Mg; (i) P. Bar, 50 μ m.

composition of mica shows variable K/(K + Na) values in the range 0.40–0.65 (Table 2). In the white band there is a wide area of mixed muscovite and silica minerals containing 2.1–5.4 wt% of alkalis, although there is almost continuous compositional variation from SiO₂ = 66 to 81 wt% with concurrent decrease of Al₂O₃ content (30–14 wt%). The mixed crystal area contains 0.5–2.2 wt% of FeO*.

Many of apatites have fluorapatite Ca₅(PO₄)₃F compositions and others have a composition between fluorapatite and hydroxylapatite (Fig. 6). Fluorapatite contains up to 4–5 wt% F with Si, Ti and Al present in minor amounts (Table 3). It is F-rich as apatite analyzed in plutonic rocks in the complex (Table 3), and those in the apatite-oxides ores (Dymek & Owens, 2001). Some of the apatites are Cl-rich replacing F. Manganous phosphate

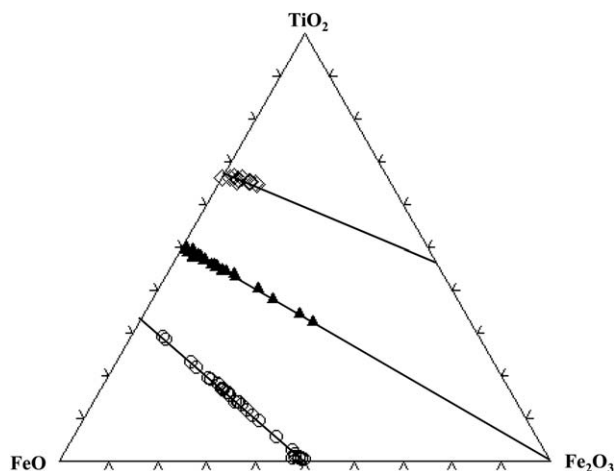


Fig. 5 Composition of Fe-Ti-oxides in the FeO*-Al₂O₃-TiO₂-rich rocks. “Ferro-pseudobrookite” shown on the join FeTi₂O₅-Fe₂TiO₅ actually consists of myrmekitic intergrowth of rutile and either ilmenite or titanomagnetite.

has MnO between 6 and 15 wt%, iron phosphate has FeO* between 6 and 37 wt%, aluminophosphate has 32–47 wt% Al₂O₃ and 9 wt% MgO (Table 3). The manganese phosphate and iron phosphate are depleted in both F and Cl, although the amounts of OH were not analyzed in the present study.

4. Whole-rock chemistry

Representative samples of the Bana FeO*-Al₂O₃-TiO₂-rich rocks and associated volcanic rocks were collected in sites 1 and 2. Globular FeO*-Al₂O₃-TiO₂-rich rocks were hand and magnet separated into globule and groundmass fractions or crushed as whole rocks. Similarly, banded FeO*-Al₂O₃-TiO₂-rich rocks were separated into iron-rich and Al-rich fractions. Al-rich fraction obtained from banded FeO*-Al₂O₃-TiO₂-rich rocks were weathered and eliminated. A total of 16 samples were selected and prepared in a tungsten-carbide mortar and crushed in an agate mortar with acetone after (careful) ultrasonic cleaning in distilled water. A total of 0.5 g of powder and 5 g of lithium tetraborate were mixed and poured into a platinum crucible in the presence of lithium bromide (trace) to create fused glass discs for X-ray fluorescence analysis. Standards were prepared from oxides Fe₂O₃, SiO₂ and Al₂O₃ reagents to obtain 100% Fe₂O₃, 100% SiO₂, 100% Al₂O₃, 50% Fe₂O₃ + 50% Al₂O₃, 50% SiO₂ + 50% Al₂O₃, 50% Fe₂O₃ + 50% SiO₂ in addition to six Geological Survey of Japan geochemical standards. Because the

FeO*-Al₂O₃-TiO₂-rich rocks have extraordinary composition, we first obtained the ternary correction parameters for SiO₂, Fe₂O₃ and Al₂O₃ from the synthetic standards, and determined the concentration of three oxides. Subordinate components other than these three oxides were then calculated utilizing usual regression method for rock analyses.

Major element compositions (SiO₂, Al₂O₃, TiO₂, FeO* (total iron as FeO), MnO, MgO, CaO, N₂O, K₂O and P₂O₅) were analyzed using X-ray fluorescence spectrometer at the Division of Earth and Environmental Sciences, Faculty of Human Development, Kobe University and at the Center for Instrumental Analysis, Yamaguchi University in Japan. Some of the trace element data were obtained using pressed powder pellets at the Geochemisches Gemeinschaftslabor, TU Berlin (Germany), and on sample discs at the Center for Instrumental Analysis, Yamaguchi University (Japan). High precision inductively coupled plasma-mass spectrometry (ICP-MS) data were also obtained on three samples (K111-glo, K111-gr, and K111) at Actlab, Ancastor, Ontario, Canada.

Analytical data for FeO*-Al₂O₃-TiO₂-rich rocks and one transitional tholeiitic basalt are shown in Table 4. The compositions were plotted in silica variation diagrams in Figure 7. The globules are enriched in FeO*, P₂O₅ and MnO compared to the groundmass. TiO₂ is mostly concentrated in the groundmass (3.2–9.2 wt%), as are SiO₂ (39–43.8 wt%) and Al₂O₃ (34.5–41.3 wt%). K₂O and Na₂O in globule and the groundmass sum to <1.2 wt% and vary between 1 and 6 wt% in the massive Al-rich FeO*-Al₂O₃-TiO₂-rich rocks. The high concentration in potassium is thought to be due to alteration. As a general feature of the FeO*-Al₂O₃-TiO₂-rich rocks, Fe₂O₃*, P₂O₅, and CaO show negative correlation with silica. TiO₂ and Al₂O₃ in globules have a negative correlation with silica, and the same oxides in groundmass and in massive Al-rich FeO*-Al₂O₃-TiO₂-rich rocks are positively correlated with silica. Figure 7 shows marked difference of the compositional trends between the FeO*-Al₂O₃-TiO₂-rich rocks and basalt-rhyolite suite of volcanic rocks (Kuepouo *et al.*, 2006) of the Bana complex. There is a compositional break in the CaO-SiO₂ and other diagrams at around SiO₂ = 50 wt%, suggesting that the FeO*-Al₂O₃-TiO₂-rich rocks have a much different origin from the associated volcanic rock suite. Table 4 also shows the density of the FeO*-Al₂O₃-TiO₂-rich rocks, which ranges from 3.4 to 3.7 g cm⁻³.

Because SiO₂, Al₂O₃, and FeO* are the major oxide components of the FeO*-Al₂O₃-TiO₂-rich rocks, we plotted the compositions of the rocks with the associated volcanic rocks in an SiO₂-Al₂O₃-FeO* ternary

Table 2 Selected compositions of aluminous minerals in the FeO*-Al₂O₃-TiO₂-rich rocks

Sample	K111	K117	K117	K117	K105	K105	K105	K105	K105	K105	K113	K111
	mk	mk	mk	mk	alu							
SiO ₂	34.47	33.10	26.09	22.30	5.36	3.50	2.17	3.44	3.68	2.77	3.58	3.58
Al ₂ O ₃	62.08	60.04	63.52	67.66	91.14	89.87	91.39	91.02	90.49	91.27	92.51	92.51
TiO ₂	0.41	0.02	0.04	0.06	0.77	0.60	0.73	0.51	0.66	0.64	2.09	2.09
FeO*	2.23	2.28	1.68	3.63	3.00	5.04	5.95	4.49	4.55	4.89	2.17	2.17
MnO	0.00	0.00	0.00	0.01	0.01	0.03	0.04	0.00	0.00	0.06	0.02	0.02
MgO	0.04	0.06	0.05	0.03	0.02	0.07	0.04	0.05	0.06	0.06	0.06	0.06
CaO	0.09	0.16	0.06	0.09	0.16	0.01	0.01	0.02	0.02	0.03	0.02	0.02
Na ₂ O	0.00	1.43	1.15	0.94	0.01	0.08	0.00	0.02	0.09	0.03	0.03	0.03
K ₂ O	0.00	2.98	3.20	2.14	0.01	0.01	0.00	0.02	0.01	0.01	0.02	0.02
P ₂ O ₅	0.79	0.20	0.09	0.19	0.41	0.17	0.13	0.15	0.12	0.11	0.03	0.03
Total	100.2	100.3	95.9	97.1	100.9	99.4	100.5	99.7	99.7	99.9	100.6	100.6
Formula	O = 5	O = 5	O = 5	O = 5	O = 3	O = 3	O = 3	O = 3	O = 3	O = 3	O = 3	O = 3
Si	0.94	0.93	0.77	0.66	0.09	0.06	0.04	0.06	0.06	0.05	0.06	0.06
Al	2.00	1.99	2.21	2.34	1.82	1.85	1.87	1.86	1.85	1.87	1.86	1.86
Ti	0.01	0.00	0.00	0.00	0.01	0.01	0.01	0.01	0.01	0.01	0.03	0.03
Fe ²⁺	0.05	0.05	0.04	0.09	0.04	0.07	0.09	0.07	0.07	0.07	0.03	0.03
Mn	0.00	0.00	0.00	0.00	0.00	0.00	0.00	0.00	0.00	0.00	0.00	0.00
Mg	0.00	0.00	0.00	0.00	0.00	0.00	0.00	0.00	0.00	0.00	0.00	0.00
Ca	0.00	0.00	0.00	0.00	0.00	0.00	0.00	0.00	0.00	0.00	0.00	0.00
Na	0.00	0.08	0.07	0.05	0.00	0.00	0.00	0.00	0.00	0.00	0.00	0.00
K	0.00	0.11	0.12	0.08	0.00	0.00	0.00	0.00	0.00	0.00	0.00	0.00
P	0.02	0.00	0.00	0.00	0.01	0.00	0.00	0.00	0.00	0.00	0.00	0.00
Total	3.02	3.16	3.21	3.23	1.98	2.00	2.01	2.00	2.00	2.01	1.98	1.98
Al/Si	2.12	2.14	2.87	3.58								
Fe ²⁺ /Al	0.03	0.03	0.02	0.04	0.02	0.04	0.05	0.03	0.04	0.04	0.02	0.02

alu, amorphous alumina; FeO*, total iron as FeO; mk, metakaolinite.

system (Iwao, 1978) (Fig. 8a). When globule and corresponding host groundmass are compared the points plot on two domains on a line with almost unit Al₂O₃/SiO₂ ratio in Figure 8(a). Compared with the Al₂O₃-TiO₂-rich rocks, the associated Bana tholeiite-hawaiite is plotted in a distinctly more SiO₂-rich part in the ternary SiO₂-FeO*-Al₂O₃ system. As a whole the chemical composition of the Al₂O₃-TiO₂-rich rocks has similarities with laterite (Fig. 8a). In comparison, the globules resemble the ferricrete compositions in the Hekpoort laterite profile in the drill core strata 1, from near Lobatsi in Botswana reported by Beukes *et al.* (2002) in terms of SiO₂, FeO* and Al₂O₃ concentrations, whereas the groundmass resembles the Fe-poor mottled zone described in the same profile in terms of SiO₂ and Al₂O₃ concentrations. It should be noted that laterites are not found around the FeO*-Al₂O₃-TiO₂-rich rocks of Bana. Iwao (1978) described the compositional fields of laterite and bauxite in the SiO₂-FeO*-Al₂O₃ system, and the compositions of the Al₂O₃-TiO₂-rich rocks, especially the globular and dark band have the compositions within the compositional field of laterite.

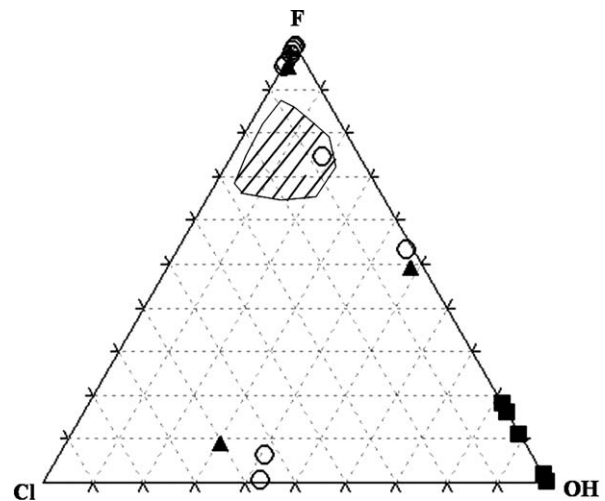


Fig. 6 OH-Cl-F proportions of phosphate minerals in the FeO*-Al₂O₃-TiO₂-rich rocks. The shaded area is the compositional field of apatite from the magnetite flow in Chile (Naslund *et al.*, 2002). (○) Apatite; (■) Al phosphate; (▲) Fe-Mn phosphate; (+) apatite in granite.

Table 4 Whole-rock analysis of the Bana FeO*-Al₂O₃-TiO₂ rich rocks

Samples	Separate globule and groundmass				Al-rich band (B)				Whole globular type				Al-rich lower zone				Host rock
	K105	K105	K111	K113	K113	KG6-OM	KG6-OM	B	K116	K117	K105	K113	Glo+Gr	K41	K46-2	KG5-OL	
	Glo	Gr	Glo	Gr	Glo	B	B		B	Glo+Gr	Glo+Gr	Glo+Gr	Al-rich	Al-rich	Al-rich	pl-basalt	
Density 10 ⁻³ kg m ⁻³						3.09											
SiO ₂ (wt %)	35.83	43.60	23.27	43.83	25.66	39.08	54.11		47.23	25.46	39.03	30.77	39.43	46.56	39.08	2.82	
TiO ₂	2.98	3.92	4.50	9.21	3.27	6.53	2.29		2.23	1.45	3.32	4.31	7.14	3.99	6.16	49.29	
Al ₂ O ₃	33.13	41.30	19.59	36.47	23.33	34.48	30.93		23.55	20.35	34.90	25.81	33.36	28.24	29.48	2.70	
FeO*	24.17	8.24	41.96	8.32	37.98	15.89	6.63		21.12	41.96	18.26	30.88	16.31	15.04	13.20	19.39	
MnO	0.12	0.08	0.06	0.02	0.12	0.07	0.02		0.04	0.08	0.11	0.11	0.07	0.01	0.01	9.48	
MgO	0.09	0.10	0.23	0.18	0.54	0.02	0.07		0.07	0.06	0.07	0.40	0.17	0.26	0.07	0.14	
CaO	0.54	0.20	1.87	0.15	1.72	0.32	0.41		0.58	1.02	0.63	1.41	0.41	0.60	0.48	2.85	
Na ₂ O	0.23	0.51	0.18	0.42	0.22	0.35	0.98		0.66	0.59	0.43	0.36	0.40	1.12	1.35	10.15	
K ₂ O	0.08	0.21	0.04	0.12	0.14	0.21	0.29		0.69	1.19	0.18	0.23	0.65	2.41	4.46	3.12	
P ₂ O ₅	0.61	0.55	1.22	0.26	1.30	0.58	0.96		0.36	0.69	0.68	1.19	0.49	0.33	0.36	0.80	
Total	97.78	98.71	92.91	98.98	94.27	97.51	96.70		96.53	92.85	97.60	95.46	98.43	98.56	94.63	99.32	
ppm																	
Ba		107.0	299.0						855	750		370	564	380	826	261	
Bi		<0.1	<0.1						<0.1	42		30					
Sr		127	391						346	130		670					
Nb		34.7	83.5						104				548	137	233	620	
Y		40.3	39.7						223				101	105	76	23	
Ga		24	49						68				92	153	88	26	
Co		60	103						29				47	56	44	6	
Mo		44	2						41							37	
Cu		108	12						75							<2	
Pb		<5	<5						12								
V		535	197						15				8	15	7	n.d.	
Zn		77	189						252				223	198	187	210	
Zr		364	611						1153				301	362	116	98	
La		5.40	93.3						67.8				759	711	623	168	
Ce		11.6	214						146							19.0	
Pr		1.32	24.9						17.0							39.4	
Nd		5.80	113						75.6							5.30	
Sm		1.49	27.2						20.2							24.0	
Eu		1.05	8.71						6.19							6.04	
Gd		2.62	25.5						24.5							2.05	
Tb		0.76	3.52						4.01							5.85	
Dy		6.40	15.1						21.4							0.85	
Ho		1.60	2.05						3.92							4.77	
Er		5.74	4.49						11.1							0.87	
Tm		0.956	0.487						1.54							2.25	
Yb		5.91	2.52						9.05							0.322	
Lu		0.897	0.298						1.36							1.86	
SUM		51.5	535.4						409.9							0.247	

†Measured at room temperature using He gas picnometer Accupyc 1330 (Shimazu Co. Ltd, Kyoto Japan).

FeO*, total iron measured as FeO. Major elements measured on X-ray fluorescence spectrometry; trace elements measured on inductively coupled plasma.

Al-rich, massive Al-rich sample from the lower zone; B, Al-rich banded layers; Glo, separate globule from the globular iron-rich sample from the upper zone; Glo+Gr, whole globule and groundmass; Gr, separate groundmass from the iron-rich globular sample; Pl-basalt, plagioclase-phynic basalt; n.d., not determined.

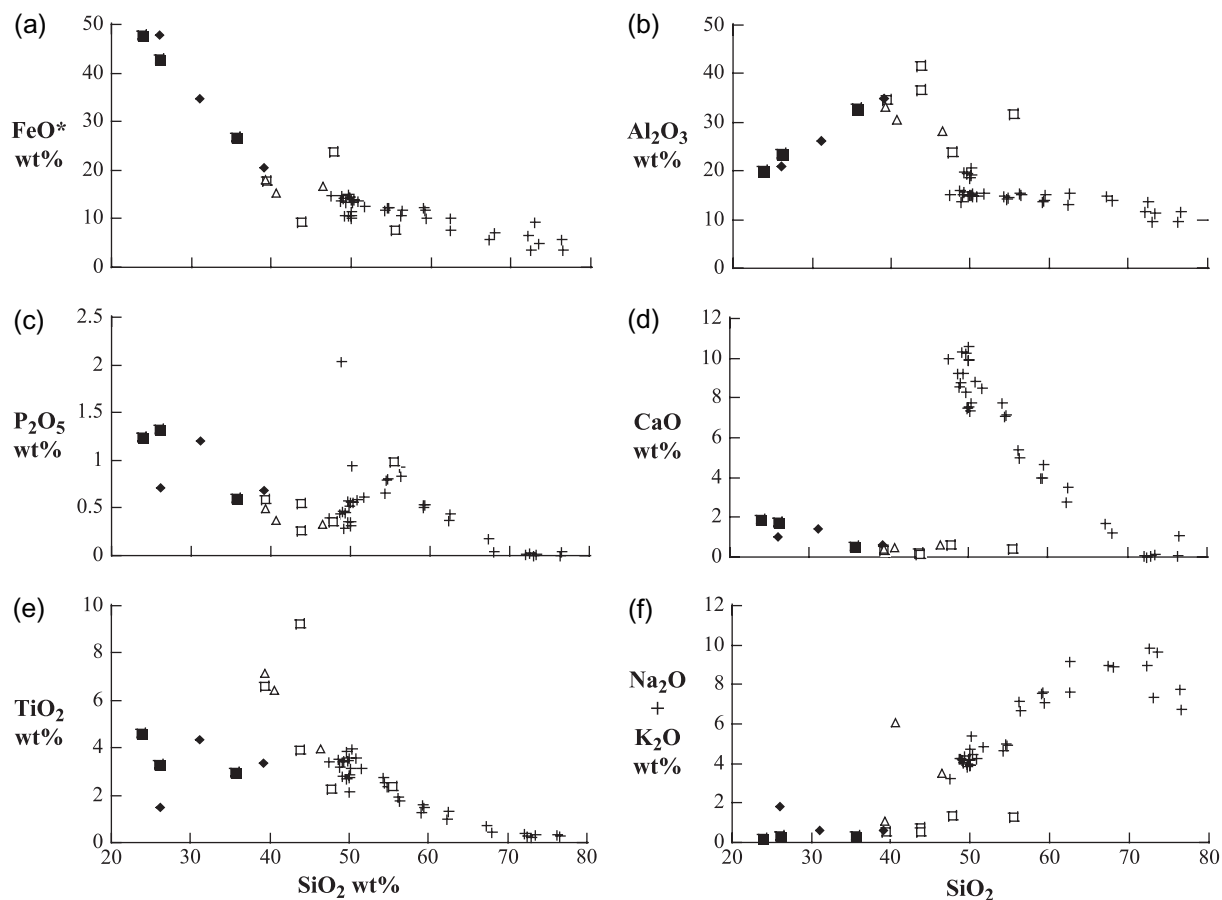


Fig. 7 Silica variation diagrams of the FeO*-Al₂O₃-TiO₂-rich rocks and associated volcanic rocks of the Tertiary Bana igneous Complex, west Cameroon. Note the compositional discrepancy between the FeO*-Al₂O₃-TiO₂-rich rocks and associated volcanic rocks in the CaO-SiO₂ diagram. It is also noted that FeO* and P₂O₅ show negative correlation with SiO₂, whereas TiO₂ and Al₂O₃ show positive correlations with SiO₂ for the FeO*-Al₂O₃-TiO₂-rich rocks. (+) Basalt-rhyolite; (□) globule; (■) groundmass; (◆) bulk ore; (△) Al-rich rocks.

In contrast, the igneous texture and the geochemical data on globules and host groundmass in some samples are apparently in agreement with pairs that may have been formed through liquid immiscibility (Philpotts, 1976; Roedder, 1978; Naslund, 1983), although these systems are not alumina-oversaturated, and the effect of which is not known. In comparison, the bordering plagioclase-phyric transitional basalts are high in TiO₂ (2–4 wt%), moderate in Fe₂O₃* (9–15 wt%), and variably high in Al₂O₃ (13–21 wt%), the highest value of which is due to accumulation of plagioclase in the most porphyritic basalts. As basalts, they are characteristically low in MgO (2–5 wt%). Clearly, the major element variation diagrams do not permit a genetic relationship between the FeO*-Al₂O₃-TiO₂-rich rocks and adjacent volcanic rocks.

Figure 8(b) shows the Al₂O₃–(CaO + Na₂O + K₂O)–(FeO* + MnO + MgO) relations of the relevant rocks. Iwao (1978) noted that “Emery” rocks containing Al₂O₃-rich minerals consistently have low (CaO + Na₂O + K₂O) component in the diagram compared with the common volcanic rocks. Figure 8(b) demonstrates that the FeO*-Al₂O₃-TiO₂-rich rocks plot within the compositional field of the Emery rocks of Iwao (1978), indicating intimate genetic connections between those rocks. Lateritic rocks of Hekpoort, Pretoria, and the Malabar coast also plot in a similar compositional field in Figure 8(b).

Highly mobile trace elements, such as Rb and Sr, are depleted in the FeO*-Al₂O₃-TiO₂-rich rocks, similar to major elements such as Na and K. Sr tends to be concentrated in the groundmass of globular

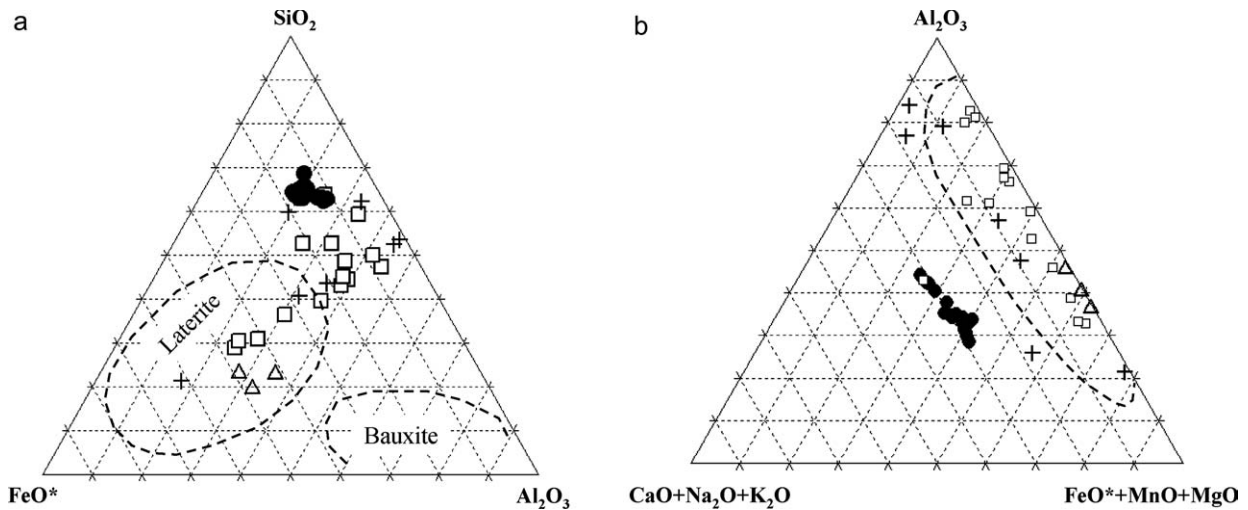


Fig. 8 (a) SiO₂-FeO*-Al₂O₃ relations of the Bana FeO*-Al₂O₃-TiO₂-rich rocks compared with the associated volcanic rocks and other lateritic compositions. (■) Bana FeO*-Al₂O₃-TiO₂-rich rocks; (●) Bana tholeiite-hawaiite (Kuepouo *et al.*, 2006); (+) laterites and related rocks of Hekpoort, Pretoria (Beukes *et al.*, 2002) and (Δ) Malabar coast, Africa (Aleva, 1994); field encircled by dashed line, laterite and bauxite (Iwao, 1978). Note nearly unit Al₂O₃:SiO₂ ratio, which corresponds to minerals such as kaolinite. (b) Al₂O₃-(CaO + Na₂O + K₂O)-(FeO* + MnO + MgO) ternary system. The FeO*-Al₂O₃-TiO₂-rich rocks are similar to the compositions of the “Emery” rocks of Iwao (1978), which are distinctly lower in the proportion of (CaO + Na₂O + K₂O) compared with the common volcanic rocks.

FeO*-Al₂O₃-TiO₂-rich rocks and in Al-rich rocks (KG5-OL, KG6-OM, K41, and K46-2). Rb does not show a regular preference for globule nor groundmass. As a consequence of their high Al content, the groundmass and Al-rich varieties of FeO*-Al₂O₃-TiO₂-rich rocks are enriched in Ga up to 68 ppm. V, Co, Cu, and Zn along with other high-field-strength elements (Zr, Y, Hf and Th) are highly concentrated in FeO*-Al₂O₃-TiO₂-rich rocks.

ICP-MS was performed on four samples: K111-globule, K111-groundmass, KG6-globule, and K111 whole globule and groundmass (Table 4). Primary mantle-normalized trace element composition indicated depletion (or negative anomaly) in Rb and Sr for all samples, except for one globule specimen (K111-glo), which had high and almost equal fractionation of La, Ce, Sr, Nd, and Sm; Nb and Ta are enriched in all samples with Ta peaks.

Chondrite-normalized rare-earth element (REE) patterns are tied (Fig. 9) and indicate variable fractionation of light REE (LREE) relative to heavy REE (HREE) ((La/Yb)_N = 20 in K111-groundmass; 0.51 in K111-glo [site 2]; 4.16 in KG6-glo [site 1]; 9.63 in the host tholeiite). The sample K111-glo has a small positive Eu anomaly. The LREE abundances of FeO*-Al₂O₃-TiO₂-rich rocks, except that of K111-glo, are enriched as compared with associated transitional tholeiitic basalt. The Ce anomaly (positive or negative), prime geochemical

evidence of alteration, is not encountered in the FeO*-Al₂O₃-TiO₂-rich rocks. Importantly, K111-glo and K111-groundmass compositions are complementary pairs on chondrite-normalized pattern, with their respective pattern crossing at Ho. As such the separate analysis of globule and groundmass of K111 globular

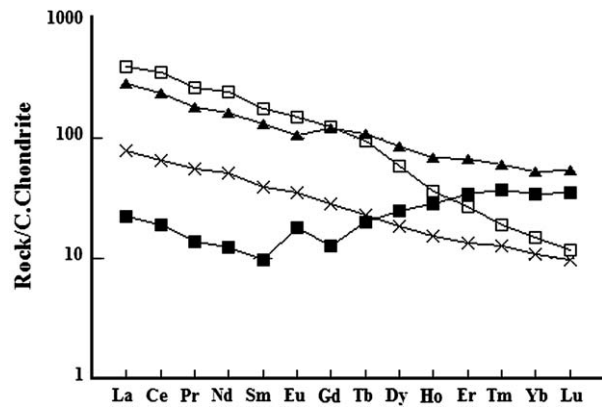


Fig. 9 Chondrite-normalized rare-earth element (REE) compositions of the FeO*-Al₂O₃-TiO₂-rich rocks. The globule and groundmass of K111 show contrasting light REE depletion and enrichment, respectively. Normalization values are from Anders and Grevesse (1989). (■) Globule; (□) groundmass; (▲) Fe-rich band; (×) host basalt. C. chondrite, carbonaceous chondrite.

FeO*-Al₂O₃-TiO₂-rich rocks suggests that LREE and MREE (middle earth rare elements from La to Dy) have a positive correlation with Al₂O₃ and TiO₂, whereas HREE have a positive correlation with FeO* and P₂O₅ (Fig. 9, Table 4).

5. Discussion and interpretations

5.1 Temperature and $f(\text{O}_2)$ estimates

Temperature and $f(\text{O}_2)$ conditions are crucial in discussing the genesis of Fe-rich rocks. Here we first describe the results of the Fe-Ti-oxide geothermometry and oxygen fugacity barometry, then discuss the constraints from mineral assemblage of the FeO*-Al₂O₃-TiO₂-rich rocks of the Bana complex. Although both magnetite-ulvospinel and ilmenite-hematite solid solution have wide compositional ranges in the FeO*-Al₂O₃-TiO₂-rich rocks, there are abundant magnetite-ilmenite contiguous grains in the globule and Fe-rich band of the FeO*-Al₂O₃-TiO₂-rich rocks (Fig. 3c), which may enable equilibrium temperature and oxygen fugacity to be determined. Utilizing the QUILF program of Anderson *et al.* (1993), we obtained the temperature and $f(\text{O}_2)$ of the analyzed contiguous pairs. Equilibration criteria of Bacon and Hirschmann (1988) were not able to be applied because of the low MnO and MgO content of both magnetite and ilmenite solid solutions. Several pairs of magnetite and ilmenite gave temperatures in a range of 693–830°C, and $\log \Delta(\text{FMQ}) = 0.95\text{--}2.18$, which is slightly oxidizing compared with those of the Ni-NiO buffer reactions. Although the presence of hematite is interpreted to be of secondary origin due to its local occurrence, presence of titanomagnetite, ilmenite and ferro-pseudobrookite in the rock should be noted. Phase equilibrium studies indicate that the ferro-pseudobrookite as analyzed (Table 1) is not stable at temperatures <800°C (Lindsley, 1991). Although the ferro-pseudobrookite actually consists of fine symplectitic Fe-Ti oxides, we suggest that the symplectite texture and the consistent compositions indicate the primary one-phase ferro-pseudobrookite in the Al₂O₃-TiO₂-rich rocks.

Coexistence of andalusite-sillimanite indicates equilibration temperatures of >550°C and pressures <400–500 MPa, which is consistent with the magnetite-ilmenite thermometry. Presence of corundum and quartz in a rock may constrain the temperature–pressure conditions (Harlov & Milke, 2002), although these minerals are not in contact, and there are Al-Si minerals such as Al₂SiO₅ and cordierite between corundum and quartz, suggesting not enough evidence for the equi-

libration of these minerals. Therefore, available mineral data indicate that the Bana FeO*-Al₂O₃-TiO₂-rich rocks were formed at 690–830°C and in low-pressure conditions with oxygen fugacity 0–1 log unit higher than NNO buffer assemblage.

5.2 Textural implications of the Bana FeO*-Al₂O₃-TiO₂-rich rocks

The Bana FeO*-Al₂O₃-TiO₂-rich rocks have some textural features encountered chiefly in igneous rocks, such as flow banding, and microlitic fluid texture in globules, outlined by the preferential concentration of andalusite and silica minerals occasionally with apatite. Polygonal through globular to banded texture of the FeO*-Al₂O₃-TiO₂-rich rocks may be due to the higher viscosity of the partially melted FeO*-rich part of the rocks, whereas the Al₂O₃-rich groundmass or bands may represent high-degree partial melting with lower viscosity. These textures may also be interpreted as being formed in an unconsolidated state of lateritic soils before heating.

Another aspect of textural features of the FeO*-Al₂O₃-TiO₂-rich rocks is the apparently gradual transition from the Al-rich basalt to the rocks. Relict pilotaxitic textures are noted in the globules and iron-rich bands, where the aluminosilicates exhibit a lath texture (Fig. 3a). These may be interpreted as having retained the original groundmass texture of basalts, later replaced by aluminosilicates and oxides by hydrothermal processes, or that lateritization retained the original groundmass texture of basalt, which was subsequently metamorphosed by the heat of basalt to form the aluminosilicates and oxides. Because the formation of the rocks requires large change of bulk rock compositions, especially enrichment of alumina, iron and titanium, hydrothermal alteration may not be likely because of the low solubility of alumina in hydrothermal water, and of the absence of sulfides in the rocks.

5.3 Similarities and differences between the Bana FeO*-Al₂O₃-TiO₂-rich rocks and iron-apatite ores

Because of the lack of such a composition in ore-geology records that limits the studies to which we can compare our data, we summarize the main hypotheses for the genesis of well-documented iron ore deposits associated with volcanic rocks before the discussion of the origin of the Bana FeO*-Al₂O₃-TiO₂-rich rocks. The

Kiruna deposits (Northern Sweden) and El Laco deposit (Chile) are the most well-known examples in this regard. The main exception is aluminum content: the Bana FeO*-Al₂O₃-TiO₂-rich rocks are much richer in Al₂O₃ than samples from Kiruna and El Laco. Neglecting this difference, some aspects of the Kiruna and El Laco ores can be useful in interpreting the data from Bana. The Kiruna ore type is considered to be magmatic in origin (Frietsch, 1978; Kolker, 1982; Nystrom & Henriquez, 1994), hydrothermal by certain authors (Barton & Johnson, 1996; Barton, 1998; Edfelt *et al.*, 2005) or exhalative-sedimentary based on field observation (erosion surface rather than intrusive contact of the wall-rock contact), textural and mineralogical data (Parak, 1975). Temperatures and oxygen fugacities of several Fe-oxide apatite ores are reported to be 600–1000°C, and 10⁻²⁰–10⁻¹¹ atm (Kolker, 1982), close to the FMQ buffer curve, which is very similar to the values of the Bana FeO*-Al₂O₃-TiO₂-rich rocks as reported in the present study. Kolker (1982) also suggested a magmatic liquid immiscibility hypothesis for the production of the iron-apatite ore based on the uniform modal proportion of iron oxide and apatite, which is similar to those of the experimental immiscible liquid. The El Laco ore type is thought by some workers to have a magmatic origin (Park, 1961; Henriquez & Martin, 1978; Hitzman *et al.*, 1992; Naslund *et al.*, 2002), others favor the hydrothermal or evaporate origins (Barton & Johnson, 1996). Arguments are based on the occurrences of the ores with the associated volcanic rocks, textural characteristics of the Fe-ore, thermometry and oxygen barometry, and bulk rock compositions. Any contribution aimed at reconstituting the origin of the Bana FeO*-Al₂O₃-TiO₂-rich rocks should take into consideration these characteristics.

5.4 Genesis of the Bana FeO*-Al₂O₃-TiO₂-rich rocks

The Bana FeO*-Al₂O₃-TiO₂-rich rocks resemble iron deposits such as Kiruna (Parak, 1975) in terms of (i) their geological setting, which usually reflects a relationship with extensional tectonic setting, and (ii) host volcanic rocks, which are intermediate to acid for Kiruna ore and El Laco (Park, 1961), and are basic to intermediate in Bana FeO*-Al₂O₃-TiO₂-rich rocks. They differ in their bulk chemical composition: the Bana FeO*-Al₂O₃-TiO₂-rich rocks have high Al₂O₃ and low MgO and CaO concentrations. Another particular feature of the Bana FeO*-Al₂O₃-TiO₂-rich rocks is that

elevated Ti generally accompanies increasing Al₂O₃ content. The concentration of major elements in FeO*-rich and Al₂O₃-rich varieties is such that the bulk compositions of the Bana FeO*-Al₂O₃-TiO₂-rich rocks can be represented by the pseudoternary systems SiO₂-FeO*-Al₂O₃ and Al₂O₃-(CaO + Na₂O + K₂O)-(FeO* + MnO + MgO). In these systems (Fig. 8) the Bana FeO*-Al₂O₃-TiO₂-rich rocks are mostly plotted in the compositional field of laterites, and much differs from liquids of mantle origin or those formed by partial melting of normal granitic, dioritic or granulitic crustal source regions. REE patterns of samples normalized to chondrite are comparable with the associated volcanic rocks, except one of the two globules analyzed on ICP-MS. But all the samples exhibit an high HREE character in Figure 9, suggesting that their REE may have been derived from the associated basaltic magmas. Cerium is an important tracer of redox condition in geologic systems, and is expressed as a Ce-negative anomaly (interaction with seawater or input of lanthanides) or Ce-positive anomaly (fractionation of Ce during oxidation and accumulated in residual rock). Absence of Ce anomaly in FeO*-Al₂O₃-TiO₂-rich rocks suggests that strong oxidation was not important during their formation. If the Bana FeO*-Al₂O₃-TiO₂-rich rocks are of igneous origin, a key question is how these rocks acquired such an unusual composition. To address this question we applied petrological approaches such as fractional crystallization of basaltic magma or partial melting of refractory materials in the crust. From the fractional crystallization viewpoint, the overall low silica content of the bulk composition of the Bana FeO*-Al₂O₃-TiO₂-rich rocks could partly be explained by iron enrichment proceeding at constant silica content during fractionation of ferro-basaltic composition. This process also explains the phosphorus and/or volatile (F, P, Cl) concentrations in the mineralized melt, but it fails to explain some features of the Bana FeO*-Al₂O₃-TiO₂-rich rocks such as Al-oversaturation and very low K, Na, and Ca content. In addition, Liu and Presnall (1990) showed that there is a thermal barrier in the system of olivine-plagioclase-silica between basalt and Al-oversaturated mineral (sapphirine) at low pressure. Even at high pressure (10–20 kbar) where the thermal barrier is suppressed, the expected mineral assemblage is spinel-sapphirine-plagioclase. Although some of the corundum occurring in basaltic rocks may have crystallized at high pressures (Sutherland *et al.*, 1998), the presence of andalusite along with corundum in the Bana FeO*-Al₂O₃-TiO₂-rich rocks indicates crystallization at low pressures, and the rocks

may not be derived from basaltic magma by magmatic processes.

As noted here, the bulk rock compositions of the FeO*-Al₂O₃-TiO₂-rich rocks are distinct from the associated volcanic rocks, and the compositional field is overlapping with laterite, suggesting that the FeO*-Al₂O₃-TiO₂-rich rocks are derived from laterite reheated and recrystallized at high temperatures. Sediments or metasediments or metalaterites could be possible sources of metalliferous mineralization in Bana. According to this reasoning, the present-day position of the complex perhaps overlaps with a fossil intracontinental basin or fault zone, which favored the mechanical and/or chemical accumulation of metals and REE from weathering of pre-existing mafic rocks. One of the candidates for the source for the Bana FeO*-Al₂O₃-TiO₂-rich rocks is deep-seated high-Ti "metalaterite". Such metalaterite has been reported from South Africa by Beukes *et al.* (2002) and from Russia by Makrygina and Petrova (1998) and from Japan (Iwao, 1978; Nishio *et al.*, 2003). Genetically, it is thought that high rates of heat derived from the rising upper mantle responsible for the lithospheric thinning (extension) and subsequent partial melting facilitated the fusion of the crustal refractory target source. The mantle-derived hot magma may also have contributed to the trace-element and REE composition of the FeO*-Al₂O₃-TiO₂-rich rocks. This crustal melt must have been F-rich, giving it a low density and viscosity and allowing it to ascend rapidly to the surface by buoyancy.

Another candidate for the source of laterite may be the Tertiary formations of laterite during the igneous activity of the Bana complex. As noted here, the bulk composition of the Bana FeO*-Al₂O₃-TiO₂-rich rocks is similar to that of modern laterite (Schellmann, 1981, 1983; Bourman, 1993; Aleva, 1994) (Figs 8, 9). Lateritization may take place rapidly in humid high-temperature conditions, and it is possible that laterite was formed in several thousand years from the older basaltic lava flows, which are subsequently overlain by hot basaltic magma pile, from which heat was supplied and recrystallization took place to form the FeO*-Al₂O₃-TiO₂-rich rocks. Concerning the stratigraphically higher position of the FeO*-Al₂O₃-TiO₂-rich rocks with the associated basaltic lavas, there are three possible interpretations of the occurrence of the rocks: (i) the FeO*-Al₂O₃-TiO₂-rich rocks were emplaced in the upper portion of the lava flow; (ii) the FeO*-Al₂O₃-TiO₂-rich rocks occupy the lower part of the lava flow with the subsequent removal of the overlying basalt body due to weathering; and (iii) the FeO*-Al₂O₃-TiO₂-rich rocks represent the

baked lower contact of basaltic lava flows, where contact metamorphism or hydrothermal alteration occurred. It seems that the first model is not likely because of the higher density of the FeO*-Al₂O₃-TiO₂-rich rocks compared with the basaltic magmas. There is no laterite at present in the Bana complex, but weathering of basaltic lava may occur after the emplacement of the lava up to the present. Concentration of FeO*-rich rocks in the upper part is consistent with the laterite profiles (e.g. Aleva, 1994; Hill *et al.*, 2000), supporting that the source laterite was formed *in situ*. At present we have limited data to constrain the definite processes of the formation of the FeO*-Al₂O₃-TiO₂-rich rocks, although we suggest that the rocks were formed by reheating of lateritic materials by the heat of hot basaltic magmas.

6. Concluding remarks

The present results show that many features of the Bana FeO*-Al₂O₃-TiO₂-rich rocks can be reconciled with recrystallization of metal-rich material such as high Ti-laterites by the heat of basaltic lavas near the surface. Mineral equilibration temperatures between 690°C and 830°C of the rocks are in accord with the recrystallization of laterite hypothesis. Unusual bulk rock chemistry of the rocks matches the compositional field of laterites in the ternary system of SiO₂-FeO*-Al₂O₃. Although the poor exposure of the rocks prevents definitive stratigraphic relationship with the surrounding volcanic rocks, the intimate occurrence of the FeO*-Al₂O₃-TiO₂-rich rocks with plagioclase-phyric basalts suggests that lateritic materials are incorporated in the basaltic magma near the surface, and together emplaced as lava flow, during which pyrometamorphic recrystallization transformed the laterite into the FeO*-Al₂O₃-TiO₂-rich rocks. This model of recycled metal-rich source in the crust may account for the genesis of some Fe-oxide ores associated with volcanic rocks occurring elsewhere.

Acknowledgments

This paper is part of the PhD work of the senior author. The authors thank Professor Makoto Watanabe and Professor Yoshiaki Tainosho, for valuable discussions. Technical advice by Dr Noritetsu Yoshida (XRD) and Dr Naotaka Tomioka (EMPA) are acknowledged. Kind comments on the earlier version of the manuscript by Professors A. R. Philpotts, M. W. Hitzman, Dr P. L.

Blevin, Dr David Cooke, Professor H. Shimazaki, and Professor M. Enami much improved the content of the paper. Thanks are also due to Professor F.M. Tchoua, Drs E. Njonfang and P. Kamgang for discussions and field trip. We thank Dr K. Suzuki-Kamata and the members of the volcanology group at Kobe University for their discussions. This study was made possible by the fellowship of MEXT (Monbukagakusho) of Japan to G. K., and by Grant-in-Aid from the JSPS to H. S.

References

- Aleva, G. J. J. (1994) Laterites. Concepts, geology, morphology and chemistry. International Soil Reference and Information Center, Wageningen, 169p.
- Anders, E. and Grevesse, N. (1989) Abundances of the elements: Meteoritic and solar. *Geochim. Cosmochim. Acta*, 53, 197–214.
- Anderson, D. J., Lindsley, D. H. and Davidson, P. M. (1993) QUILF: A PASCAL program to assess equilibria among Fe-Mg-Mn-Ti oxides, pyroxenes, olivine, and quartz. *Comput. Geosci.*, 19, 1333–1350.
- Bacon, C. R. and Hirschmann, M. M. (1988) Mg/Mn partitioning as test for equilibrium between coexisting Fe-Ti oxides. *Am. Mineral.*, 73, 57–61.
- Barton, M. D. (1998) Evaluation of possible roles of non-magmatic brines in igneous-related hydrothermal systems, especially Fe (-Cu-Au-REE) deposits. Abstract Geological Society of America Annual meeting, Toronto, Ontario. A-127.
- Barton, M. D. and Johnson, D. A. (1996) Evaporite-source model for igneous-related Fe oxide (REE-Cu-Au-U) mineralization. *Geology*, 24, 259–262.
- Beukes, N. J., Dorland, H., Gutzmer, J., Nedachi, M. and Ohmoto, H. (2002) Tropical laterites, life on land, and the history of atmospheric oxygen in the Paleoproterozoic. *Geology*, 30, 491–494.
- Bourman, R. P. (1993) Perennial problems in the study of laterite: A review. *Aust. J. Earth Sci.*, 4, 387–401.
- Carmichael, I. S. E. (1967) The iron-titanium oxides of salic volcanic rocks and their associated ferromagnesian silicates. *Contrib. Mineral. Petrol.*, 14, 36–64.
- Deer, W. A., Howie, R. A. and Zussman, J. (1992) An introduction to the rock-forming minerals, 2nd edn. Longman, London, 687p.
- Droop, G. T. R. (1987) A general equation for estimating Fe³⁺ concentrations in ferromagnesian silicates and oxides from microprobe analyses, using stoichiometric criteria. *Mineral. Mag.*, 51, 431–435.
- Dymek, R. F. and Owens, B. E. (2001) Petrogenesis of apatite-rich rocks (nelsonites and oxide-apatite gabbro-norites) associated with massif anorthosites. *Econ. Geol.*, 96, 797–815.
- Edfelt, A., Armstrong, R. N., Smith, M. and Martinsson, O. (2005) Alteration paragenesis and mineral chemistry of the Tjarrojakka apatite-iron and Cu (-Au) occurrences, Kiruna area, northern Sweden. *Mineral. Deposita*, 40, 409–434.
- Fitton, J. G. (1987) The Cameroon line, west Africa: A comparison between oceanic and continental alkaline volcanism. In Fitton, J. G. and Upton, B. G. J. (eds) Alkaline igneous rocks. Geological Society, London, Special Publication No. 30, 273–291.
- Frietsch, R. (1978) On the magmatic origin of iron ores of the Kiruna type. *Econ. Geol.*, 73, 478–485.
- Harlov, D. F. and Milke, R. (2002) Stability of corundum+quartz relative to kyanite and sillimanite at high temperature and pressure. *Am. Mineral.*, 87, 424–432.
- Henriquez, F. and Martin, R. F. (1978) Crystal growth textures in magnetite flows and feeder dykes, El Laco, Chile. *Can. Mineral.*, 16, 581–589.
- Hill, I. G., Worden, R. H. and Meighan, I. G. (2000) Geochemical evolution of a palaeolaterite: The Interbasaltic formation, Northern Ireland. *Chem. Geol.*, 166, 65–84.
- Hitzman, M. W., Oreskes, N. and Einaudi, M. T. (1992) Geological characteristics and tectonic setting of Proterozoic iron oxide (Cu-U-Au-REE) deposits. *Precambrian Res.*, 58, 241–287.
- Iwao, S. (1978) Re-interpretation of the chloritoid-, staurolite- and emery-like rocks in Japan: Chemical composition, occurrence and genesis. *J. Geol. Soc. Jpn.*, 84, 49–67.
- Kolker, A. (1982) Mineralogy and geochemistry of Fe-Ti oxide and apatite (nelsonite) deposits and evaluation of the liquid immiscibility hypothesis. *Econ. Geol.*, 77, 1146–1158.
- Kuepou, G. (2004) Geology, petrology and geochemistry of the Tertiary Bana volcano-plutonic complex, west Cameroon, central Africa (PhD Thesis). Kobe University, Kobe, Japan. 301p.
- Kuepou, G., Tchouankoue, J. P., Nagao, T. and Sato, H. (2006) Transitional tholeiitic basalts in the Tertiary Bana volcano-plutonic complex, Cameroon Line. *J. Afr. Earth Sci.*, 45, 318–332.
- Lindsley, D. H. (1991) Experimental studies of oxide minerals. *Rev. Mineral.*, 25, 69–106.
- Liu, T. C. and Presnall, D. C. (1990) Liquidus phase relationships on the join anorthite-forsterite-quartz at 20 kbar with applications to basalt petrogenesis and igneous sapphirine. *Contrib. Mineral. Petrol.*, 104, 735–742.
- Makrygina, V. A. and Petrova, Z. I. (1998) The importance of geochemical data for geodynamic reconstruction: Formation of the Olkhon metamorphic complex, Lake Baikal, Russia. *Lithos*, 43, 135–150.
- Moreau, C., Regnault, J. M., Déruelle, B. and Robineau, B. (1987) A new tectonic model for the Cameroon Line, Central Africa. *Tectonophys.*, 139, 317–334.
- Naslund, H. R. (1983) The effect of oxygen fugacity on liquid immiscibility in iron-bearing silicate melts. *Am. J. Sci.*, 283, 1034–1059.
- Naslund, H. R., Henriquez, F., Nystrom, J. O., Vivallo, O. and Dobbs, F. M. (2002) Magmatic iron ores and associated mineralisation: examples from the Chilean High Andes and Coastal Cordillera. In Porter, T. M. (ed.) Hydrothermal iron oxide copper-gold and related deposits: A global perspective 2. PGC Publishing, Adelaide, 207–226.
- Nishio, D., Minagawa, T. and Noto, S. (2003) Emery from Ko-Oge Island in Ryoke terrane, Seto Inland Sea, Japan. *Jpn. Mag. Mineral. Petrol. Sci.*, 32, 165–174 (in Japanese with English abstract).
- Nystrom, J. O. and Henriquez, F. (1994) Magmatic features of iron ores of the Kiruna type in Chile and Sweden: Ore textures and magnetite geochemistry. *Econ. Geol.*, 89, 820–839.
- Parak, T. (1975) Kiruna iron ores are not 'intrusive-magmatic' ores of the Kiruna type. *Econ. Geol.*, 70, 1242–1258.
- Park, C. F. (1961) A magnetite "flow" in Northern Chile. *Econ. Geol.*, 56, 431–436.

- Philpotts, A. R. (1976) Silicate liquid immiscibility: Its probable extent and petrogenetic significance. *Am. J. Sci.*, 276, 1147–1177.
- Poudjom Djomani, Y. H., Nnange, J. M., Diament, M., Ebinger, C. J. and Fairhead, J. D. (1995) Effective elastic thickness and crustal thickness variations in west-central Africa inferred from gravity data. *J. Geophys. Res.*, 100, 22 047–22 070.
- Poudjom Djomani, Y. H., Diament, M. and Wilson, M. (1997) Lithospheric structure across the Adamawa plateau (Cameroon) from gravity studies. *Tectonophys.*, 273, 317–327.
- Roedder, E. (1978) Silicate liquid immiscibility in magmas and in the K_2O - FeO - Al_2O_3 - SiO_2 : An example of serendipity. *Geochim. Cosmochim. Acta*, 42, 1597–1617.
- Schellmann, W. (1981) Considerations on the definition and classification of laterites. *In Proceedings of the International Seminar on Lateritisation Processes*, Trivandrum, India. A.A Balkema, Rotterdam, 1–10.
- Schellmann, W. (1983) A new classification of laterite. *Nat. Resour. Dev.*, 18, 7–21.
- Sutherland, F. L., Hoskin, P. W. O., Fanning, C. M. and Coenraads, R. R. (1998) Models of corundum origin from alkali basaltic terrains: A reappraisal. *Contrib. Mineral. Petrol.*, 133, 356–372.
- Toteu, S. F., Van Schmus, W. R., Penaye, J. and Nyobe, J. B. (1994) U-Pb and Sm-Nd evidence for Eburnian and Pan-African high grade metamorphism in cratonic rocks of southern Cameroon. *Precambrian Res.*, 67, 321–347.
- Turnock, A. C. and Eugster, H. P. (1962) Fe-Al-oxides: Phase relationships below 1000°C. *J. Petrol.*, 3, 533–565.